IEEE Access
Multidisciplinary | Rapid Review | Open Access Journal

Received January 15, 2019, accepted February 7, 2019, date of publication February 19, 2019, date of current version March 7, 2019.

Digital Object Identifier 10.1109/ACCESS.2019.2900161

Implementation of a Battery-Free Wireless Sensor for Cyber-Physical Systems Dedicated to Structural Health Monitoring Applications

GAËL LOUBET[1], ALEXANDRU TAKACS[1,2], (Member, IEEE), AND DANIELA DRAGOMIRESCU[1,3], (Senior Member, IEEE)

[1]LAAS-CNRS, Université de Toulouse, 31031 Toulouse, France
[2]UPS, Université de Toulouse, 31062 Toulouse, France
[3]INSA, Université de Toulouse, 31077 Toulouse, France

Corresponding author: Gaël Loubet (gael.loubet@laas.fr)

This work was supported in part by the French National Research Agency (ANR) through the McBIM Project (Communicating Material at the disposal of the Building Information Modeling) under Grant ANR-17-CE10-0014, and in part by the Region Occitanie in the frame of OPTENLOC Research Project.

ABSTRACT This paper addresses the concept of a wirelessly powered and battery-free wireless sensor for the cyber–physical systems dedicated to the structural health monitoring applications in harsh environments. The proposed material architecture is based on a smart mesh wireless sensor network composed of sensing nodes and communicating nodes. The sensing nodes are used to sense the physical world. They are battery-free and wirelessly powered by a dedicated radiofrequency source via a far-field wireless power transmission system. The data collected by the sensing nodes are sent to the communicating nodes that, between others, interface the physical world with the digital world through the Internet. A prototype of the sensing node—using a LoRaWAN uplink wireless communication and temperature and relative humidity sensor—has been manufactured, and the experiments have been performed to characterize it. The experimental results prove that the periodicity of measurement and communication can be controlled wirelessly by using only the wireless power transmission downlink. In this paper, we highlight the performance of this complete implementation of a wirelessly powered and battery-free wireless sensing node—not yet integrated or miniaturized—designed for implementing complete cyber–physical systems and based on the simultaneous wireless information and power transfer. Finally, an investigation of comparable implementations of the battery-free sensing nodes for the cyber–physical systems is carried out.

INDEX TERMS Cyber-physical systems (CPS), Internet of Things (IoT), wireless power transmission (WPT), wireless sensor network (WSN), simultaneous wireless information and power transfer (SWIPT), communicating materials.

I. INTRODUCTION

Internet of Things (IoT) technologies have generated many opportunities in the field of Cyber-Physical Systems (CPS) for Structural Health Monitoring (SHM) applications [1], especially for building, civil and transportation infrastructures [2]. In harsh environments [3] deploying Wireless Sensor Networks (WSN) induces some hard requirements including a long, reliable and maintenance-free lifespan because of the inaccessibility of the sensors once installed.

The associate editor coordinating the review of this manuscript and approving it for publication was Remigiusz Wisniewski.

Regarding these hypotheses, an innovative WSN architecture was recently introduced in [3] within the scope of the McBIM (Material communicating with the Building Information Modeling) project [4], which will provide a reinforced communicating concrete. This communicating reinforced concrete must be able to generate, process, store and exchange data with other structural elements and with a Building Information Modeling (BIM) to keep up to date. Thus, it is a Cyber-Physical System, which can be used in the manufacturing, construction and exploitation phases of the lifecycle of civil infrastructures, especially for Structural Health Monitoring applications.

The proposed WSN is composed of a smart mesh network of two kinds of nodes: the Sensing Nodes (SNs) and the Communicating Nodes (CNs).

The Sensing Nodes are able to sense the physical world (i.e. the monitored structure) and communicate the collected data from their environments to the Communicating Nodes over a distance ranging from several meters to kilometers, bespoke to the targeted application. The issues concerning installation and maintenance costs are considered, as well as the need of a system that can reliably operate for decades without being accessible. Thus, to avoid any maintenance and to increase the lifetime, the Sensing Nodes are designed to be battery-free and wirelessly powered by a RF power source driven by (or even integrated into) CNs through a Wireless Power Transmission (WPT) interface. As communication and WPT work on the same frequency band, this implementation answers the paradigm of Simultaneous Wireless Information and Power Transfer (SWIPT) [5] and [6].

The Communicating Nodes are able to accumulate, process, store and exchange data generated by their associated SNs. They are accessible and do not need to be energy autonomous for their entire lifetime. The CNs are also gateways to the digital world (the Internet) by using, for instance, a 'nG' cellular network interface. No complete implementation of the Communicating Nodes is currently proposed. Thus, the used LoRa gateway and RF power source can be considered as an exploded CN. Also, routing protocols which will be used for the data exchanges between CNs and algorithms which will be implemented in CNs are not considered here. Finally, data processing and storing algorithms through the Internet, servers and BIM are not treated in this article. Only the Sensing Nodes implementation as part of a complete Cyber-Physical System is discussed.

In this paper, we propose an original and innovative wirelessly powered and battery-free implementation of a wireless Sensing Node. This SN will operate as part of a complete CPS and is wirelessly powered by using a far-field WPT approach. Moreover, the periodicity of measurements and wireless communication is controlled by a well-tuned use of the WPT. Indeed, the need of measurements can change during the targeted lifetime (several decades) of the system and cannot be fully specified during the design phase.

Section II introduces the architecture of the Sensing Nodes, as well as the specifications of the implemented prototype. Experimental results (obtained in controlled and real environments) for the innovative concept related to CPS SNs implementation (the command of the measurements and wireless communication periodicity through the WPT interface) are presented in Section III. The inherent constraints of the proposed prototype as well as its potential improvements are discussed in Section IV.

II. SENSING NODES: TOPOLOGY AND DESIGN

The Sensing Nodes are dedicated to the generation of data by sensing their environmental and/or internal properties (e.g. temperature, humidity, etc.). These measured data are sent to the associated CN(s) through a unidirectional radiofrequency communication. The SNs must be low power and as simple as possible, therefore no data are stored in them. To meet the needs in terms of lifetime (decades) and maintenance (SNs are inaccessible) these must be battery-free and energy autonomous. Consequently a WPT system (i.e. a RF source), integrated into and/or only commanded by the CNs, is implemented to power wirelessly the SNs. By modulating the total amount of power transferred to SNs, the CNs can manage the periodicity of measurements and transmission of the associated SNs.

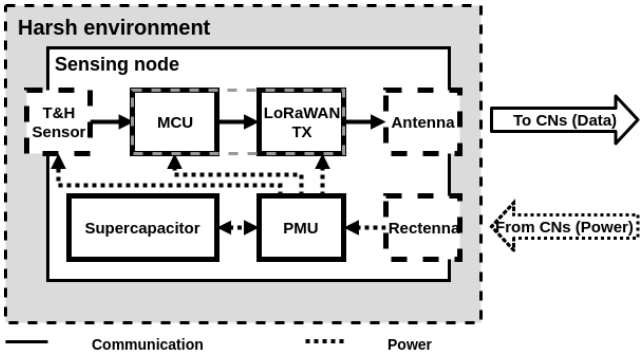

FIGURE 1. Schematic diagram for the architecture of the wireless sensing node.

The topology of the implemented SN for CPS is presented in Fig. 1. It consists of:

(i) a temperature and humidity (T&H) sensor, sensing the temperature and relative humidity of its environment.
(ii) a development board containing a MicroController Unit (MCU) and a LoRaWAN transceiver (TX) with a dedicated antenna. This board processes and transmits the collected data by the T&H sensor to the CNs.
(iii) an in-house designed rectenna with reflector, acting as a WPT interface and recovering RF power from CNs to provide dc power.
(iv) a Power Management Unit (PMU), embedding a dc-to-dc convertor and managing (storing and delivering) the available energy, provided by the rectenna. The energy is stored in a supercapacitor and used by the T&H sensor, the MCU and LoRaWAN transceiver.
(v) a supercapacitor (22 mF) acting as an energy storage element charged and discharged by the PMU in the active components.

Fig. 2 shows a photo of a proof-of-concept implementation of the Sensing Node. At this stage of the research project the prototype is neither integrated or miniaturized but it allows a proof-of-concept validation of the architecture highlighted in Fig. 1.

Our prototype of the sensing node -designed as a proof-of-concept of the adopted architecture- implements the following functionalities:

(i) the autonomy in terms of energy is assured by the WPT interface, the energy storage element and the power management unit.

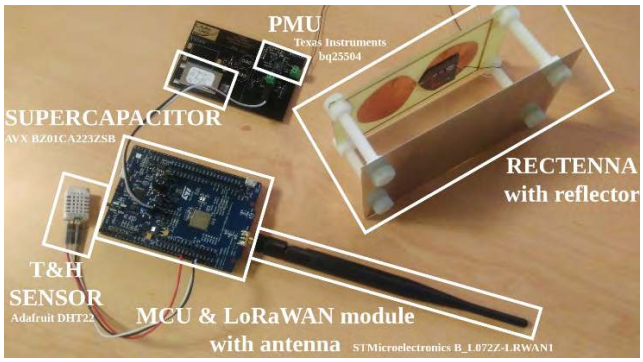

FIGURE 2. Photograph of the sensing node prototype used for experiments.

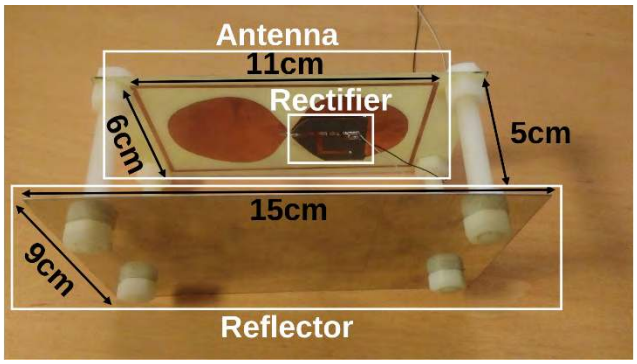

FIGURE 3. Photograph of the manufactured rectenna.

(ii) the sensing is assured by a temperature and relative humidity sensor. The values of temperature and relative humidity are binary encoded and available at the input of the MCU.
(iii) the sensing data are sent to the CNs through a wireless unidirectional radiofrequency communication following LoRaWAN standard, providing the wireless sensor has enough energy to perform a complete data frame transmission.
(iv) the reconfigurability is assured by the control and the tune of the transmitted power by CNs *via* the WPT interface: the periodicity of the measurements and communication can be controlled.

It must be noted that the capabilities of the WPT system are limited today mainly by regulations (i.e. the maximum Effective Isotropic Radiated Power (EIRP) that can be radiated in the ISM bands is limited [7]) and not by the technology itself.

A. RECTENNA: A WIRELESS POWER TRANSFER INTERFACE

In order to ensure the energy autonomy of the sensing nodes, which is one of the main constraints for the targeted application –communicating concrete for SHM of buildings, civil and transportation infrastructures-, many approaches can be followed. For instance, [8] made a review of the available energy sources and of the best strategies to harvest them in buildings for SHM applications. In order to operate efficiently for decades and in harsh environments as required by our scenario/application, the ambient energy sources are too low, too fluctuating and sometimes unavailable.

Thus, we chose the strategy of the RF Wireless Power Transmission. There are two solutions for this approach:

(i) the magnetic/near-field WPT, used by [9], [10], or [11].
(ii) the far-field RF WPT, which we have chosen.

This second solution can increase the useful range between SNs and the RF sources -the CNs- and is able to control the whole power transmission chain. By controlling the frequency and the amount of transmitted power, we can impose a periodicity of operation for the SNs and accurately estimate the system efficiency for a given scenario [12].

In order to scavenge the generated RF fields for the WPT, a specially designed rectenna (acronym from ***rec***tifying an***tenna***) [13] and [14] was tuned to operate around the ISM 868 MHz frequency band. This rectenna is presented in Fig. 3. It has a maximum simulated (by using HFSS software) gain of +6.6 dBi and is composed of:

(i) a compact broadband dipole antenna (enclosed by a rectangular ring, manufactured on FR4 substrate -thickness: 0.8 mm, relative electric permittivity: 4.4 and loss tangent: 0.02-) which captures the low ambient -and generated- electromagnetic energy field and converts it into a RF signal,
(ii) a single Schottky diode (Avago HSMS 2850 mounted in series configuration) high-frequency rectifier (manufactured on Rogers RT/Duroid 5870 substrate -thickness: 0.787 mm, relative electric permittivity: 2.3 and loss tangent: 0.0012- and connected with the antenna in parallel plan to have a 2-dimensional rectenna) which converts the guided RF signal into the dc power,
(iii) a reflector in order to increase the antenna gain (from +2.2 dBi -that is the gain of the flat dipole antenna without any reflector [14]- to +6.6 dBi -when the metallic reflector is added-) while having a 3-dimensional structure comparable at the 3D rectenna use in [3].

The rectifying process generates undesirable harmonics at the input and output ports of the diode (nonlinear device). At the input port of the rectifier, an impedance matching circuit (composed of a bent short-circuited stub and an inductor of 33 nH) acts as a band-pass filter to prevent the re-radiation by the antenna of these harmonics, and thus, maximizes the power conversion efficiency. A low-pass filter is used to provide a dc signal to the load. More details concerning the design and the characterization of the rectenna are reported in [13] and [14].

To improve the rectenna efficiency, we used a reflector positioned at 5 cm behind it and measuring 9 cm × 15 cm. In this way, the directivity and the gain of the antenna are increased in the opposite direction with the respect of the added reflector. The results depicted in Fig. 4 demonstrate

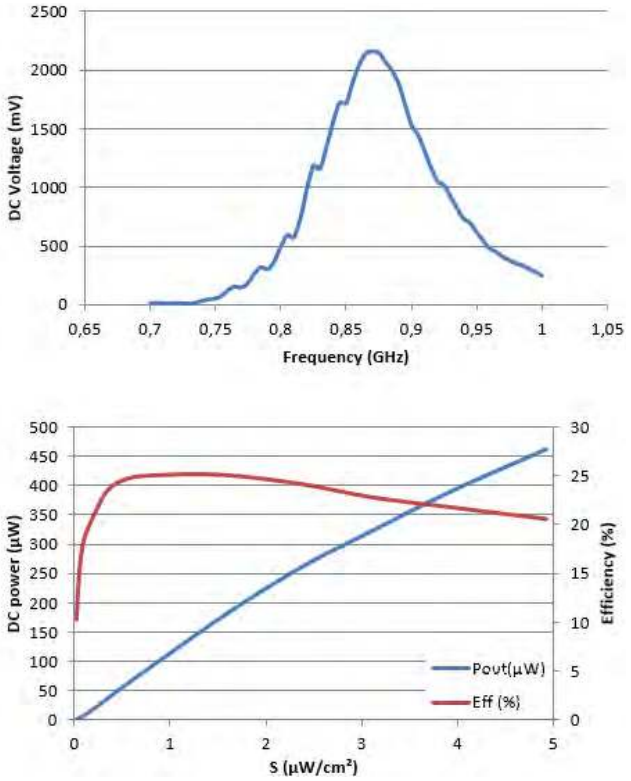

FIGURE 4. Measured rectenna performances: a) dc voltage versus frequency (load: 10 kΩ, input power: +0 dBm), b) dc power and power conversion efficiency versus illuminating power densities (frequency: 868 MHz, load: 10 kΩ).

that the manufactured rectenna operates efficiently for low power densities of the incident RF waves. A dc power greater than 50 μW can be harvested as long as the incident power density exceeds 0.4 μW/cm^2. Moreover, this rectenna is relatively broadband, covering ISM 868/915 MHz frequency band and part of the GSM bands.

B. POWER MANAGEMENT UNIT

The dc signal provided from the power harvested by the rectenna is driven toward the PMU to supply it and to be stored in an energy storage element. We choose the Texas Instruments bq25504 [15] for the PMU. It embeds a dc-to-dc convertor and requires an input power of at least 15 μW. Its role is to charge efficiently an energy storage element with the available power and to supply the entire system (the sensor, the MCU and the wireless communication unit) by discharging the energy storage element when enough energy is stored. To optimize its operation, a Maximum Power Point Tracking (MPPT) hardware function was implemented. The PMU stores power until the voltage at the ports of the energy storage element is higher than a selected threshold (V_{max} = 5.25 V) and supplies the active components until this voltage is lower than another selected threshold (V_{min} = 2.30 V). Moreover, both over- and under-voltage protections are available and used by the PMU. When the (under-) over-voltage threshold is reached the load and the energy storage element are disconnected in order to prevent the deep (dis)charge of the energy storage element. Fig. 5. shows this operational behavior.

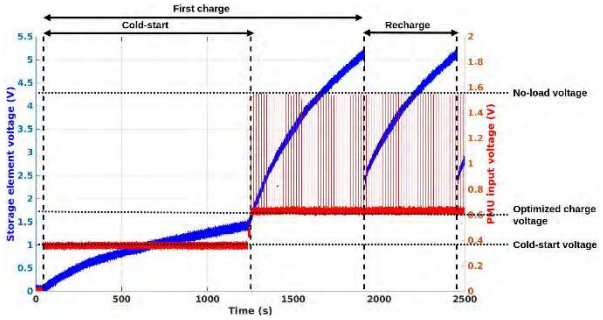

FIGURE 5. Voltage waveforms at the output ports of the energy storage element (blue) and rectenna output voltage (red), for a −8 dBm RF power at the input of the rectifier.

The largest amount of dc power is required by the transmitter device during the transmission of data collected from the sensor(s) and processed by the MCU, as presented in Fig. 6. Hopefully, in most of the scenarios, the measurements will not need to be performed continuously (e.g. the temperature and the humidity should be measured hourly or once a day/week, etc.).

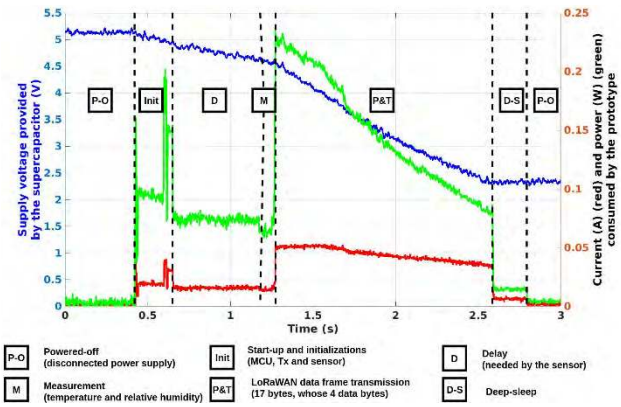

FIGURE 6. Supply voltage (blue), current consumption (red), and power consumption (green) of the load.

C. ENERGY STORAGE

We chose a supercapacitor of 22 mF (noted C) (AVX BZ01CA223ZSB [16] with a low loss current of 10 μA) as the energy storage element to store the energy harvested by the rectenna. The charges and discharges of the supercapacitor are managed by the PMU. The energy stored in the supercapacitor is used to supply the sensor, MCU and LoRaWAN transceiver module. The energy stored (noted E) by the supercapacitor can be estimated as:

$$E = \frac{C}{2} \cdot \left(V_{max}^2 - V_{min}^2 \right) \quad (1)$$

By using eq. (1), the energy stored by a 22 mF supercapacitor is estimated to 245 mJ. The measured consumption

TABLE 1. Comparative study of four wireless communication technologies identified as possible solutions for the transceiver unit of the sensing nodes.

Technology	Standard	Directionality	Frequency (ISM)	Range	Minimal frame size (byte)	Module	Manufacturer	DC consumption in Tx mode (mW)
LoRa (far-field)	LoRaWAN [22]	Uplink ; (Downlink restricted)	433/868/915 MHz	Long (km)	14	CMWX1ZZABZ-091 [19]	Murata	119 at +10 dBm & 3.3 V (typ)
Bluetooth Low Energy (BLE) (far-field)	IEEE 802.15.1 [23]	Bidirectional ; "Uplink only" available	2.4 GHz	Middle (dozen of m)	11	QN908x [24]	NXP	12 at 0 dBm & 3 V (typ)
RFID (near-field or far-field)	ISO/IEC 18000 [25]	Uplink by interrogation / backscattering	13.56 kHz; 433 MHz; 860-960 MHz; 2.45 GHz	Short (dozens of cm)	7	SL900A [26]	AMS	6.9 at 3 V (max)
RuBee (near-field)	IEEE 1902.1 [27]	Essentially bidirectional	131 kHz (65 kHz for WPT)	Middle (dozen of m)	5	N/A	N/A	N/A

of the SN prototype for the collect, process and transmission of a measurement is around 214 mJ as presented in Fig. 6. Thus, a 22 mF supercapacitor (maximum charging voltage $V_{max} = 5.25$ V and minimum allowed discharging voltage $V_{min} = 2.30$ V) can store enough energy to supply our system during all its processing time.

D. LORAWAN DEVELOPMENT BOARD: MCU AND WIRELESS COMMUNICATION MODULE

Because of the availability of a reliable infrastructure in our laboratory and the ease of development, we selected the LoRa technology and LoRaWAN protocol as the solution for the unidirectional radiofrequency communication link between SNs and CNs. Through it, we can perform a long-range wireless communication between our prototype and the LoRa gateway installed on INSA campus (Toulouse, France, GPS coordinates: 43° 34'14.8''N 1° 27'58.5''E), located at 1.3 km away from the prototype (LAAS-CNRS Toulouse, France, GPS coordinates: 43° 33'45.3''N 1° 28'38.4''E). The data generated and transmitted by the SN are then routed by the TheThingsNetwork [17] network, up to servers, where we can recover and process them. As said previously, routing protocols and data processing and storage algorithms are not treated in this paper.

We use the development board STMicroelectronics B-L072Z-LRWAN1 [18] that contains an all-in-one LoRaWAN communication module Murata CMWX1ZZABZ-091 [19], composed of:

(i) a STMicroelectronics STM32L072CZ [20] MCU based on an ARM Cortex M0+,
(ii) a Semtech LoRa transceiver SX1276 [21].

The transceiver manages the LoRa physical layer protocol, whereas the MCU manages the LoRaWAN protocol stack and the application software.

The processing and communication parts are simplified as much as possible. Thus, four bytes of data (provided by the sensor) are recovered and transmitted each time when the system is supplied. The length of the transmitted frame is set at 17 bytes (there are 13 bytes dedicated to the protocol in a LoRaWAN frame and 4 bytes of data). The transmission respects LoRaWAN class A standards (the node sends data but it cannot be interrogated), with a +2 dBm radio frequency output power at 868 MHz (ISM band), an activation by personalization (ABP), and without causing an acknowledgment from the network. This all aids to limit the number of exchanges, and reduce power consumption. The bandwidth is 125 kHz, and the spreading factor is 12, allowing a data-rate of 293 bps. It is likely that this configuration can be further optimized.

Regarding the application constraints, the choices of the LoRa technology and LoRaWAN protocol are not necessarily the most appropriate. The need for the communication between SNs and CNs can be defined as a unidirectional uplink communication over distances between a few of meters and hundreds of meters. Table 1 shows a comparison between four technologies (LoRaWAN, Bluetooth Low Energy, RFID and RuBee) identified as possible solutions to implement the wireless communication unit of the SNs for different communication range (long, middle and short). We must notice that the RuBee technology is based on near-field communication and is not yet commercially available. Moreover, a dedicated frequency for WPT is defined in its standard. To complete Table 1, we have to take into consideration the duration of transmissions (and of eventual receptions, if control frames are needed) to estimate precisely the consumption of each standard and module presented.

E. TEMPERATURE AND RELATIVE HUMIDITY SENSOR

We generate data to be transmitted through an active temperature and relative humidity sensor (Adafruit DHT22 [28]). Each quantity is coded on 2 bytes and has a respective sensitivity of 0.1 °C and 0.1 %.

This sensor is not low-power (it was selected mainly by its availability and facility of use/programing in order to have a quick proof-of the concept of our approach). It needs a stabilized supply voltage between 3 V and 5 V. The dedicated protocol implemented for it requires switching on the sensor one second before performing any measure. Two seconds are needed between each measurement. Thus, it is an active sensor that is slow and therefore more power consuming. Moreover, it is not dedicated to harsh environments. Thus, we could not embed it in concrete for instance. Next, we must choice low-power -maybe passive- sensors which could be used in diverse hard environments. Nevertheless, having a functional prototype with this sensor means that we can have a more optimal system in the future.

F. PROTOTYPE COMPLETE OPERATION

First if the energy storage element is empty, the PMU is switched-on by using a cold start-up procedure, which requires an input voltage higher than 350 mV and a dc power higher than 15 μW. Otherwise, when the cold-start is achieved, the PMU charges efficiently the energy storage element. Once enough stored energy is available, the active components are supplied. Thus, the supercapacitor is charged and discharged between two threshold voltages, as presented in Fig. 5. Specifically, the software initializes the MCU, the sensor -with a delay of almost one second before being usable-, and the wireless communication module. Then the prototype senses temperature and relative humidity, and makes a LoRaWAN transmission, before being deactivated and shifting to a deep-sleep mode before being powered-off. As presented in Fig. 6, the treatment lasts approximately 2.13 s (830 ms to initialize the system and make a measurement, and 1.30 s to transmit a data frame). The system needs at least 214 mJ to work properly, as detailed earlier. The recovering, processing and storing of data on the servers has not yet been implemented. We only visually checked on a web-browser for a good reception of data.

III. EXPERIMENTAL RESULTS

We split the experiments into three steps. Firstly, we characterized our prototype with a controlled power at the input of the rectifier, and thus without a rectenna and WPT. Secondly, we tested the prototype in an anechoic chamber with its rectenna and a RF power transmitter used as the controlled RF source. Finally, we tested our system in a real environment in order to set an easier communication with the LoRa gateway.

To generate an electromagnetic power density that illuminates the rectenna and can supply the prototype, we used a RF source composed of a power synthesizer (Anritsu MG3694B, operating at 868 MHz) and a patch antenna with a maximal gain of +9.2 dBi. The losses due to the connection cables and connectors between synthesizer and antenna are estimated at 2.5 dB. As transmission and WPT frequency bands are the same (868 MHz) we use linear polarized antennas in orthogonal polarizations to discriminate RF WPT and communication. Thus, we implement a functional solution for the SWIPT paradigm. The voltage measurements are performed by using a LeCroy WaveRunner 6100 oscilloscope.

A. PROTOTYPE SUPPLIED BY A CONTROLLED RF POWER AT THE INPUT OF ITS RECTIFIER

To characterize the prototype, a RF signal generator (Anritsu MG3694B), operating at 868 MHz, was directly connected at the input ports of the RF rectifier (equipped with a SMA connector). The same rectifier, used here as a standalone device, is also integrated in the rectenna, as presented in section II.A. The cold-start voltage (to be provided by the rectifier) required to switch on the PMU is around 350 mV. This voltage can be generated if the RF power at the input of the rectifier is higher than −10 dBm. The cold-start duration is a function of the RF power at the input of the rectifier. When a RF power of −8 dBm is injected at the input of the rectifier, the cold-start lasts 3 h 33 min and the first charge is 5 h 16 min. When a RF power of +0 dBm is injected at the input of the rectifier, the cold-start lasts 17 min 51 s and the first charge is 29 min 04 s. Fig. 5 shows a typical voltage waveform observed at the ports of the supercapacitor for a complete processing from an empty energy storage element. Fig. 7 and Table 2 show the evolution of the measurement and transmission periodicity and the output dc voltage of

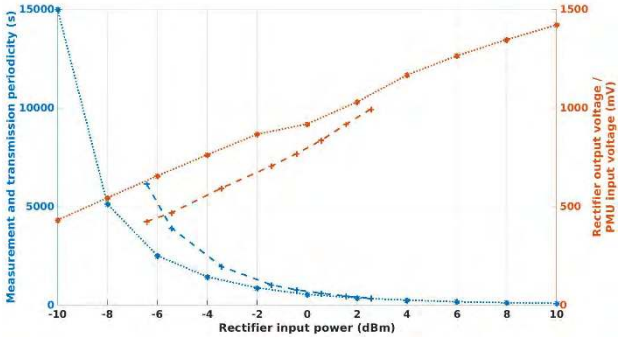

FIGURE 7. Measurement and transmission periodicity (blue) and rectifier output voltage (orange) in function of the applied RF input power for the prototype supplied by a controlled RF power at the input of the rectifier (∗), by a controlled power density illuminating the rectenna in an anechoic chamber (+). In this case, the RF power at the input of the rectifier is estimated by taking into account the simulated gain of the antenna integrated into the rectenna.

TABLE 2. Characteristics of the sensing node supplied with a controlled RF power at the input of the rectifier.

Rectifier input power (dBm)	Rectifier output voltage (mV)	Measurements periodicity
-10	431	~ 4 h
-8	544	~ 1 h 25 min
-6	655	~ 41 min 30 s
-4	762	~ 23 min 51 s
-2	866	~ 14 min 30 s
0	918	~ 9 min 13 s
2	1030	~ 6 min 03 s
4	1166	~ 4 min 10 s
6	1264	~ 2 min 51 s
8	1346	~ 1 min 58 s
10	1421	~ 1 min 24 s

the rectifier as a function of the RF power at the input port of the rectifier. As depicted in Table 2 and Fig. 7, we can control the periodicity of measurements and transmission of our prototype by controlling the amount of RF power at the input of the rectifier (or alternatively by controlling properly the power density illuminating the rectenna). This periodicity can be between 1 min 24 s (+10 dBm) and nearly 4 h (−10 dBm once cold-start achieved).

Thus, we are able to modify the periodicity of measurement and communication without changing the hardware or the software of the CPS SN, just by controlling the transmitted RF power.

B. PROTOTYPE SUPPLIED BY A CONTROLLED RF POWER DENSITY ILLUMINATING THE RECTENNA IN AN ANECHOIC CHAMBER

Experiments with a complete WPT interface were performed in an anechoic chamber, as presented in Fig. 8, to avoid any interference or multipath effects. The SN is located at 150 cm from the RF WPT source, so in the far field region. The RF power density that illuminates the rectenna under testing can be computed as:

$$S = \frac{d^2}{3600.\pi.P_T.G_T} \tag{2}$$

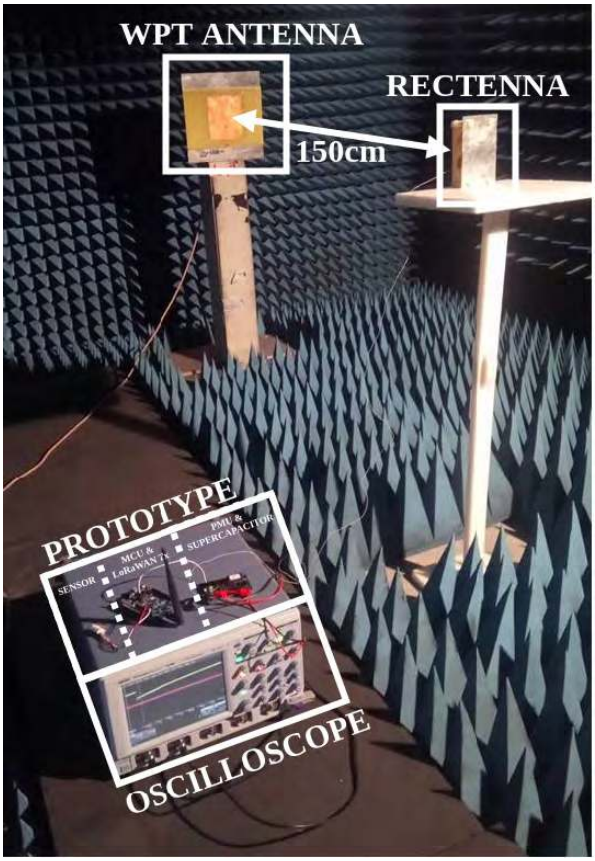

FIGURE 8. Photograph of our experimental setup (SN powered by using a WPT technique) in an anechoic chamber.

where P_T is the power generated by the RF power synthesizer, G_T the transmission patch antenna gain and d is the distance between the power transmitter and the rectenna. The RF power collected by the rectenna is computed as:

$$P_{RF} = G_r.\frac{\lambda^2}{4.\pi}.S \tag{3}$$

where G_R is the gain of the antenna integrated in the rectenna and λ the wavelength.

The results are presented in Table 3 and Fig. 7.

TABLE 3. Characteristics of the SN supplied by RF WPT in an anechoic chamber.

EIRP (dBm)	Power density (μW/cm²) [computation]	Rectifier input power (dBm) [computation]	Rectifier output voltage (mV)	Measurements periodicity
21.7	0.52	-6.43	424	~ 1 h 43 min
22.7	0.66	-5.43	468	~ 1 h 06 min
24.7	1.04	-3.43	593	~ 32 min 38 s
26.7	1.65	-1.43	705	~ 17 min 04 s
27.7	2.08	-0.43	767	~ 12 min 47 s
28.7	2.62	+0.56	835	~ 9 min 59 s
29.7	3.30	+1.56	917	~ 7 min 34 s
30.7	4.16	+2.56	994	~ 5 min 41 s

According to (2) and (3), we can generate a power density of 1 μW/cm^2 at 399 cm away from a +33 dBm EIRP source.

As we test our system in an anechoic chamber, we cannot validate the good reception of the LoRaWAN frame. Nevertheless, the prototype was powered for the duration needed to accomplish all the application software and the transmitted frequency spectrum was displayed through a vector analyzer placed in the anechoic chamber.

We were able to modulate the period of measurement and communication by controlling the EIRP of the RF source. In our experiments, the period between two consecutive processes was modulated between nearly 5 min 41 s (S = 4.16 μW/cm^2) and 1 h 43 min (S = 0.52 μW/cm^2).

As presented in Fig. 7, results obtained during the two measurements are consistent. The differences are due to the errors in the estimation of the RF power at the input of rectifier (that is -in this case- integrated into the rectenna). This RF input power is estimated by taking into account the simulated gain (around +6.6 dBi, HFSS simulation) of the antenna integrated into the rectenna and the eventual mismatching and/or mutual coupling between the rectifier and the antenna. Moreover, the MPPT changes the input impedance of the PMU in order to optimize the power transfer and generally induces a lower input voltage.

C. PROTOTYPE SUPPLIED BY A CONTROLLED RF POWER DENSITY ILLUMINATING THE RECTENNA IN A REAL ENVIRONMENT

At the date of submission, we have not obtained all the results for this third step of experimentation.

To validate the LoRaWAN communication between the prototype and the gateway -impossible from the anechoic chamber- we relocate the experimental setup in a more compliant location. Some received frames are presented in Fig. 9 for a power density irradiating the rectenna estimated at 5.5 μW/cm^2 and an input power at the input of the rectifier estimated at -0.6 dBm. These results were obtained for the prototype using the 3D rectenna, without the reflector and with a lower gain ($+2.2$ dBi). The periodicity of the measurements is less stable and varies between 26 min and 42 min due to the real environment (multi-path effects, possible RF interferences, etc.).

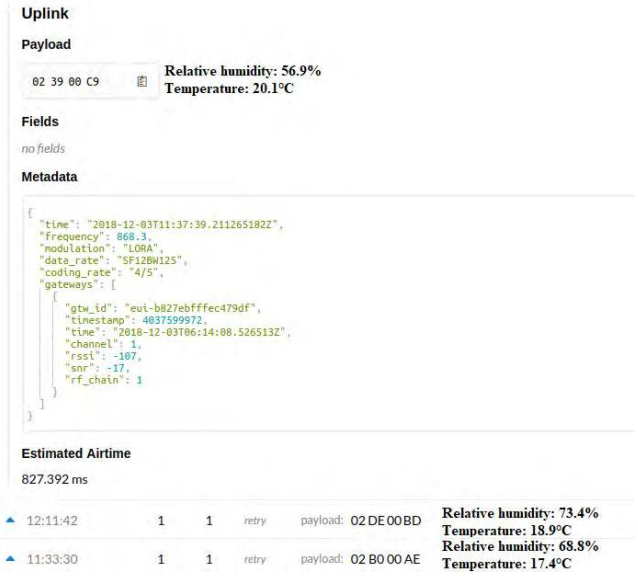

FIGURE 9. Screenshot of TheThingsNetwork interface after receiving checked frames, when the SN was illuminated with a power density of 5.5 μW/cm^2 through the 3D rectenna during experimentation in a real environment.

IV. DISCUSSIONS

The prototype of the sensing node has been designed as a proof of concept of a wirelessly powered and battery-free wireless Sensing Node for SHM application in harsh environments. The energy autonomy of the SNs is obtained by using a Wireless Power Transmission technique, which can be tuned to control the periodicity of measurement and communication. The communication is long range and based on the LoRa technology and the LoRaWAN protocol. Our SN prototype can be improved in order to be more complete, efficient, compact and relevant for the targeted applications. The work in SN prototype improvement is in progress at submission time and the main areas for improvement are presented in Section IV.B.

A. EVOLUTION OF OUR PROTOTYPE

With regards to the prototype presented in [3], some improvements have been added. Firstly, the power management has been improved by incorporating a supercapacitor with lower capacitance (22 mF for this work instead of 30 mF in [3]), which exhibits lower losses during charging time. The different thresholds that control the charges and discharges were also optimized to improve the energy use. Moreover, a temperature and relative humidity sensor was added, thus implementing a complete CPS SN but at the cost of increasing the overall dc consumption of the system. Some software improvements were processed too, especially to integrate and interrogate efficiently the sensor. Thus, as compared with [3], we have a SN for CPS, which consumes more energy (because it performs measurements) but needs a lower energy storage element thanks to optimized power management. Finally, for a comparable volume (6 cm $\times$ 11 cm $\times$ 7 cm (462 cm^2) [3] versus 9 cm $\times$ 15 cm $\times$ 5 cm (675 cm^2) in this work including the size of the reflector plane), we use a rectenna with a higher gain than in [3]. In both cases, the antenna is composed of a compact (6 cm $\times$ 11 cm) and broadband dipole antenna enclosed by a rectangular ring. In [3] a 7 cm-long rectifier was orthogonally connected to the antenna. In this work, a more compact rectifier is connected directly (in a parallel manner) on the backside of the compact flat dipole antenna. A reflector (9 cm $\times$ 15 cm) was positioned at 5 cm behind the antenna to increase the gain by $+4.4$ dB (from $+2.2$ dBi to $+6.6$ dBi). Thanks to this higher gain, the system can be supplied with a lower power density irradiating the rectenna.

B. IMPROVEMENTS AND FUTURE WORKS

The consumption of the LoRaWAN module could be eventually reduced by changing the configurations (e.g. bandwidth, spreading factor, etc.) according to gateway specifications.

Regarding the energy management aspect, we can implement some improvements in order to optimize efficiency and limit losses. For our application, we have to design a specific rectenna optimized for the load of the PMU. This is very challenging because the input impedance of the selected PMU changes dynamically as a function of the power management strategy and the energy stored in the storage element (supercapacitor). An accurate estimation of the necessary power and better defined activation thresholds could allow for decreased energy storage capacitance, allowing a more compact system that needs less input RF power to be completely charged. To be more efficient, we could add an ultra-low power voltage regulator at the PMU output in order to have a constant voltage to supply the load. It could minimize the consumption of the LoRaWAN module because the higher the input voltage, the higher the consumption current.

In addition, we must notice that the oscilloscope measurements induce losses. The input impedance of the oscilloscope is about 1 MΩ. That says: for a maximum measured voltage of 5.25 V, a power of 27.6 μW is lost (5.3 μW for 2.30 V, the minimum voltage authorized for the storage element before being disconnected from the load).

The use of a unique antenna -both for the WPT and the communications- could allow a high gain of compactness.

TABLE 4. Comparative study of implementations of LoRa sensor nodes supplied by energy harvesting system.

Ref Year	Energy source	Communication protocol	Energy management and storage	Sensor type / processing technology	Data length (byte)	Periodicity of transmission	Application
[30] 2016	Oversized emulated low power sources (between 1.5 mW and 4.2 mW) with buffers (4.7 mF and 1 mF)	LoRaWAN	PMICs (STMicroelectronis SPV1050) with switches and MCU Battery (34.7 mF)	Generic platform Wi6labs / MCU	N/A	N/A	N/A
[31] 2016	Vibration (piezoelectric electromagnetic vibration energy harvester)	LoRaWAN	PMIC (Linear Technology LTC3588) Supercapacitor (100 mF/330 mJ)	Temperature and rain Vehicles counter / MCU	8	Estimated at 3 h 30 min	Bridge SHM
[32] 2017	Backscattering and other source (Backscatter system)	LoRaWAN	Switches and FPGA OR Dedicated IC	N/A / FPGA	8	N/A (opportunistic system)	SHM; Precision agriculture; Smart contact lens; Flexible epidermal patch sensor
[33] WULoRa 2017	Solar or thermal (Solar panel or thermocouple)	OOK and GFSK	PMU (Texas Instruments bq25570) Battery (Li-Ion) Wake-up radio system	Light (ISL29023), humidity and temperature (SHT21), temperature (TMP006), atmospheric pressure (BMP180) and displacement (MPU-915) / MCU	2	N/A	N/A
[34] 2018	Electric induction (Current transformer and rectifier)	LoRaWAN	PMIC Superapacitor (22 mF)	Electricity consumption/AC current (indirect measurement) (57PR1673) / MCU	N/A	Few seconds	Smart grid
[35] 2018	Solar and battery (Solar panel with buffer supercapacitor (2 F))	LoRaWAN	PMIC (STMicroelectronis SPV1040) Battery (1400 mAh) NFC/RFID tag Wake-up radio system	Crackmeter (detection and location) (magnet and Hall effect sensor) (57PR1673) / MCU	N/A	N/A	SHM of construction material
[36] 2018	Solar and thermal (Solar panels and thermoelectric generators)	Homemade	PMIC Battery (20 Ah)	Temperature, humidity and pH / MCU	4	Hour	Environment monitoring (floating device on water)
[37] PLoRa 2018	Backscattering and solar (Backscatter system and solar panel)	LoRaWAN	PMIC Supercapacitor (33 mF) Packet detector	N/A / FPGA	284	Estimated at 20 min (opportunistic system)	N/A
This work McBIM 2019	RF WPT (Rectenna)	LoRaWAN	PMU (Texas Instruments bq25504) Supercapacitor (22 mF/245 mJ)	Temperature and humidity (DHT22) / MCU	4	Controlled by the WPT interface (minutes to hours)	Communicating material (concrete); SHM in harsh environment

Concerning the sensing part, we must adopt a low-power-maybe passive- sensor dedicated to harsh environments. Moreover, temperature and relative humidity are not always the most relevant parameters and other sensors (e.g. mechanical stress, corrosion, etc.) must also be integrated bespoke to application.

TABLE 5. Comparative study of sensor nodes supplied by RF wireless power transfer or RF energy harvesting.

Ref Year	Energy source (distance with the source / frequencies / minimal input power (dBm))	Energy storage element (capacitance)	Communication technology (frequency / range)	Sensor type	Periodicity of transmission
[38] 2010	Far field RF energy harvesting from TV broadcast (hundreds of meters or kilometers / VHF and UHF / N/A)	Aluminum electrolytic capacitor (100 µF)	SimpliciTI (2.4 GHz / tens of meters)	Temperature and voltage	5 s
[39] 2011	Far field RF energy harvesting from ambient sources (ISM band) (meters / 866 MHz / N/A)	Capacitor (6.8 µF)	Backscattering (866 MHz / N/A)	No	Opportunistic system
[40] 2012	Far field RF energy harvesting from ambient sources (ISM band) (meters / 2.45 GHz / -11)	Battery (N/A)	N/A (433 MHz / meters)	Temperature and humidity	45 s
[41] 2013	Far field RF energy harvesting from TV broadcast or cellular base (hundreds of meters or kilometers / VHF and UHF / -18)	Ceramic capacitor (160 µF)	N/A (2.4 GHz / meters)	Temperature and luminosity	[1 min; 4 min 30 s]
[42] E-WEHP 2013	Far field RF energy harvesting from TV broadcast (hundreds of meters or kilometers / [512 MHz-566 MHz] / -14.6)	Multi-layer ceramic capacitor (100 µF)	No (N/A / N/A)	No	N/A
[43] 2016	Far field RF power transfer from RFID receiver (meters / 868 MHz / -8)	Ceramic capacitors bank (1.8 mF)	BLE (2.4 GHz / meters)	Temperature	30 min
[9] 2017	Inductive WPT (centimeters / 100 kHz / N/A)	LiPo battery (N/A)	M-BUS (169 MHz / hundreds of meters)	Stress and temperature	When supply
[44] 2018	Far field RF power transfer from dedicated RF source (tens of centimeters / 868 MHz / N/A)	Capacitor (1 mF)	Bluetooth (2.45 GHz / meters)	(Temperature and voltage)	[5 s; 20 s]
[45] 2018	Far field RF WPT from dedicated RF source (meters / 868 MHz / N/A)	Tantalum capacitors (N/A)	BLE (2.4 GHz / meters)	3-axis accelerometer; temperature and humidity	0.5 s
This work McBIM 2019	Far field RF WPT from dedicated RF source (meters / 868 MHz / -8)	Supercapacitor (22 mF)	LoRa and LoRaWAN (868 MHz / kilometers)	Temperature and humidity	Controlled by the WPT interface (minutes to hours)

Finally, the proposed exploded implementation is neither integrated or miniaturized. The limitation in terms of size is function of the size of antennas and rectenna, MCU, LoRaWAN transceiver and PMU, and supercapacitor volumes.

We selected here, for our prototype, the LoRaWAN protocol standard for the wireless communication. This choice was motivated by the available infrastructure in our laboratory and by the long-range communication capability of the LoRa technology. The choice of the communication technology is a function of the following criteria:

(i) the targeted communication range between SNs and CNs,
(ii) the low-power consumption in both active (measurement, processing and transmission) and deep-sleep modes,
(iii) the possibility to allow (only) an unidirectional communication (from SN to CN), thus reducing the dc consumption of the SN,
(iv) the bit rate and frequency bandwidth (for instance this is not a relevant criterion for our targeted application [3]).

BLE or RuBee could be relevant solutions (alternative to LoRaWAN) for middle range applications.

C. RELATED WORKS REGARDING LORA NODES WITH ENERGY HARVESTING APPROACHES

As presented in Table 4, since the last two years many experiments were conducted according to energy harvesting for LoRa and LoRaWAN WSN. Some sources were exploited as solar [33], [35], [36], mechanical (vibration) [31], thermal [33], [36], inductive [34], etc. In addition, multiple sources architectures were proposed in [30], [32], [35], and [36]. All these solutions cover a large variety of applications, especially for SHM. Moreover, backscattering approaches were investigated and conceptually proved in [32] and [37].

Although the feasibility of WPT for LoRaWAN node was demonstrated theoretically in [29], to the authors' knowledge no complete implementation was provided until [3].

Our solution presents the lowest capacitance for the energy storage element (22 mF in this work and in [34]) without the inherent limitations of ambient energy harvesting approach (availability and fluctuation of the ambient energy sources) but with the need of a controlled RF source.

D. RELATED WORKS CONCERNING WSN BASED ON RF WPT OR ENERGY HARVESTING

During the last decade, WSN supplied by RF WPT or energy harvesting were studied. Some complete or partial implementations regarding SHM and smart metering (for home, environment, etc.) are presented in Table 5. These projects provide a large variety of solutions by using different RF sources (TV broadcast, cellular bases, dedicated RF sources, etc.), sensors (temperature, humidity, mechanical stress, etc.) and wireless communication technologies (backscattering, BLE, etc.).

Although they are widely employed and could be included in this comparative study, RFID solutions are not discussed here because of the limited communication range (typically tens of centimeters and few meters in the best cases) in ISM 868 MHz band. There are diverse implementations for SHM applications, especially through tags which are active [46] or intrinsically able to sense [47].

Our solution presents a complete implementation of a SWIPT system in the 868 MHz ISM band by using the LoRaWAN technology with a good compromise in terms of energy and communication range. Moreover, the periodicity of measurement and communication can be controlled by the RF source (or equivalently by controlling the amount of the RF power density illuminating the rectenna of the SN).

V. CONCLUSION

A Wireless Sensor Network was proposed for Structural Health Monitoring applications in harsh environments. It consists of a meshed grid composed of wirelessly powered and battery-free Sensing Nodes and Communicating Nodes. We developed and tested a low-power battery-free wireless sensing node able to sense relative humidity and temperature. This information was transmitted over a kilometer through a unidirectional LoRaWAN communication. This wireless sensing node is autonomous in terms of energy and is powered by far-field RF Wireless Power Transmission. Through the Wireless Power Transmission interface, it is possible to control the functionality (switch on/off) of the sensing node and its measurements and communication periodicity.

ACKNOWLEDGMENT

The authors would like to thank the help of Alassane Sidibe and Dr. Abderrahim Okba from LAAS-CNRS Toulouse for developing the rectenna structures integrated into the WPT interface of the sensing node prototypes and for their valuable help during experiments.

We acknowledge all our partners in the McBIM project, especially FINAO SAS/360SmartConnect for providing well-defined use-cases.

REFERENCES

[1] M. Z. A. Bhuiyan, J. Wu, G. Wang, J. Cao, W. Jiang, and M. Atiquzzaman, "Towards cyber-physical systems design for structural health monitoring: Hurdles and opportunities," *ACM Trans. Cyber-Phys. Syst.*, vol. 1, no. 4, pp. 1–19, 2017.

[2] A. B. Noel, A. Abdaoui, T. Elfouly, M. H. Ahmed, A. Badawy, and M. S. Shehata, "Structural health monitoring using wireless sensor networks: A comprehensive survey," *IEEE Commun. Surveys Tuts.*, vol. 19, no. 3, pp. 1403–1423, 3rd Quart., 2017.

[3] G. Loubet, A. Takacs, and D. Dragomirescu, "Towards the design of wireless communicating reinforced concrete," *IEEE Access*, vol. 6, pp. 75002–75014, 2018.

[4] *McBIM Research Project*. Accessed: Jan. 14, 2019. [Online]. Available: http://www.agence-nationale-recherche.fr/en/anr-funded-project/?tx_lwmsuivibilan_pi2%5BCODE%5D=ANR-17-CE10-0014

[5] I. Krikidis, S. Timotheou, S. Nikolaou, G. Zheng, D. W. K. Ng, and R. Schober, "Simultaneous wireless information and power transfer in modern communication systems," *IEEE Commun. Mag.*, vol. 52, no. 11, pp. 104–110, Nov. 2014.

[6] T. D. P. Perera, D. N. K. Jayakody, S. Chatzinotas, and V. Sharma, "Wireless information and power transfer: Issues, advances, and challenges," in *Proc. IEEE 86th Veh. Technol. Conf. (VTC-Fall)*, Sep. 2017, pp. 1–7.

[7] *Electromagnetic Compatibility and Radio Spectrum Matters (ERM); Short Range Devices (SRD) Intended for Operation in the Bands 865 MHz to 868 MHz and 915 MHz to 921 MHz; Guidelines for the Installation and Commissioning of Radio Frequency Identification (RFID) Equipment at UHF*, document ETSI TR 102 436, V2.1.1, ETSI, 2014.

[8] J. W. Matiko, N. J. Grabham, S. P. Beeby, and M. J. Tudor, "Review of the application of energy harvesting in buildings," *Meas. Sci. Technol.*, vol. 25, no. 1, 2014, Art. no. 012002.

[9] L. Gallucci *et al.*, "An embedded wireless sensor network with wireless power transmission capability for the structural health monitoring of reinforced concrete structures," *Sensors*, vol. 17, no. 11, p. 2566, 2017.

[10] Y. Jang, J. K. Han, J. I. Baek, G. W. Moon, J. M. Kimand, and H. Sohn, "Novel multi-coil resonator design for wireless power transfer through reinforced concrete structure with rebar array," in *Proc. IEEE 3rd Int. Future Energy Electron. Conf., ECCE Asia (IFEEC-ECCE Asia)*, Jun. 2017, pp. 2238–2243.

[11] O. Jonah and S. V. Georgakopoulos, "Wireless power transfer in concrete via strongly coupled magnetic resonance," *IEEE Trans. Antennas Propag.*, vol. 61, no. 3, pp. 1378–1384, Mar. 2013.

[12] A. Costanzo and D. Masotti, "Smart solutions in smart spaces: Getting the most from far-field wireless power transfer," *IEEE Microw. Mag.*, vol. 17, no. 5, pp. 30–45, May 2016.

[13] A. Okba, A. Takacs, and H. Aubert, "900 MHz miniaturized rectenna," in *Proc. IEEE MTT-S Wireless Power Transf. Conf.*, Montreal, QC, Canada, Jun. 2018, pp. 1–4.

[14] A. Okba, A. Takacs, and H. Aubert, "Compact flat dipole rectenna for IoT applications," *Prog. Electromagn. Res. C*, vol. 87, pp. 39–49, Sep. 2018.

[15] Texas Instruments. *BQ25504 Ultra Low-Power Boost Converter With Battery Management for Energy Harvester Applications*. Accessed: Jan. 14, 2019. [Online]. Available: http://www.ti.com/lit/ds/symlink/bq25504.pdf

[16] AVX. *BestCap Ultra-Low ESR High Power Pulse Supercapacitors*. Accessed: Jan. 14, 2019. [Online]. Available: http://datasheets.avx.com/BestCap.pdf

[17] *TheThingsNetwork*. Accessed: Jan. 14, 2019. [Online]. Available: https://www.thethingsnetwork.org/

[18] STMicroelectronics. *B-L072Z-LRWAN1*. Accessed: Jan. 14, 2019. [Online]. Available: https://www.st.com/en/evaluation-tools/b-l072z-lrwan1.html

[19] *Murata: LoRa Module Data Sheet*. Accessed: Jan. 14, 2019. [Online]. Available: https://wireless.murata.com/RFM/data/type_abz.pdf

[20] STMicroelectronics. *STM32L072x8 STM32L072xB STM32L072xZ*. Accessed: Jan. 14, 2019. [Online]. Available: https://www.st.com/resource/en/datasheet/stm32l072v8.pdf

[21] Semtech. *LoRa—SX1276/77/78/79*. Accessed: Jan. 14, 2019. [Online]. Available: https://www.semtech.com/products/wireless-rf/lora-transceivers/SX1276

[22] LoRa Alliance Technical Committee, Beaverton, OR, USA. (2017). *LoRaWAN 1.1 Specification*. Accessed: Jan. 14, 2019. [Online]. Available: https://lora-alliance.org/sites/default/files/2018-04/lorawantm_specification_-v1.1.pdf
[23] *IEEE Standard for Information Technology—Telecommunications and Information Exchange Between Systems—Local and Metropolitan Area Networks-Specific Requirements—Part 15.1: Wireless Medium Access Control (MAC) and Physical Layer (PHY) Specifications for Wireless Personal Area Networks (WPANs)*, IEEE Standard 802.15.1, IEEE 802.15.1 Working Group, 2005.
[24] *NXP: QN908x: Ultra Low Power Bluetooth 5 System-on-Chip Solution*. Accessed: Jan. 14, 2019. [Online]. Available: https://www.nxp.com/docs/en/nxp/data-sheets/QN908x.pdf
[25] *Information Technology—Radio Frequency Identification for Item Management—Part 6: Parameters for Air Interface Communications at 860 MHz to 960 MHz General*, ISO/IEC 18000-6:2013, ISO/IEC Standard 18000, ISO/IEC JTC 1/SC 31 Automatic Identification and Data Capture Techniques Technical Commitee, 2013.
[26] AMS. *SL900A*. Accessed: Jan. 14, 2019. [Online]. Available: https://ams.com/documents/20143/36005/SL900A_DS000294_5-00.pdf/d399f354-b0b6-146f-6e98-b124826bd737
[27] *IEEE Standard for Long Wavelength Wireless Network Protocol*, IEEE Standard 1902.1, IEEE 1902.1 Working Group, 2009.
[28] Sparkfun. *Digital-Output Relative Humidity & Temperature Sensor/Module—DHT22*. Accessed: Jan. 14, 2019. [Online]. Available: https://www.sparkfun.com/datasheets/Sensors/Temperature/DHT22.pdf
[29] S. Tjukovs, J. Eidaks, and D. Pikulins, "Experimental verification of wireless power transfer ability to sustain the operation of LoRaWAN based wireless sensor node," in *Proc. IEEE Adv. Wireless Opt. Commun. (RTUWO)*, Nov. 2018, pp. 83–88.
[30] P.-D. Gleonec, J. Ardouin, M. Gautier, and O. Berder, "Architecture exploration of multi-source energy harvester for IoT nodes," in *Proc. IEEE Online Conf. Green Commun. (OnlineGreenComm)*, Nov./Dec. 2016, pp. 27–32.
[31] O. Francesco, C. B. Mezzetti, and F. Cottone, "Vibrations powered LoRa sensor: An electromechanical energy harvester working on a real bridge," in *Proc. IEEE Sensors*, Oct. 2016, pp. 1–3.
[32] V. Talla, M. Hessar, B. Kellogg, A. Najafi, J. R. Smith, and S. Gollakota, "Lora backscatter: Enabling the vision of ubiquitous connectivity," *Proc. ACM Interact., Mobile, Wearable Ubiquitous Technol.*, vol. 1, no. 3, pp. 1–24, 2017.
[33] M. Magno, F. A. Aoudia, M. Gautier, O. Berder, and L. Benini, "WULoRa: An energy efficient IoT end-node for energy harvesting and heterogeneous communication," in *Proc. Conf. Design, Autom. Test Eur.*, Mar. 2017, pp. 1532–1537.
[34] G. Dalpiaz, A. Longo, M. Nardello, R. Passerone, and D. Brunello, "A battery-free non-intrusive power meter for low-cost energy monitoring," in *Proc. IEEE Ind. Cyber-Phys. Syst. (ICPS)*, May 2018, pp. 653–658.
[35] T. Polonelli, D. Brunelli, M. Guermandi, and L. Benini, "An accurate low-cost Crackmeter with LoRaWAN communication and energy harvesting capability," in *Proc. IEEE 23rd Int. Conf. Emerg. Technol. Factory Autom. (ETFA)*, vol. 1, Sep. 2018, pp. 671–676.
[36] W. K. Lee, M. J. W. Schubert, B.-Y. Ooi, and S. J.-Q. Ho, "Multi-source energy harvesting and storage for floating wireless sensor network nodes with long range communication capability," in *IEEE Trans. Ind. Appl.*, vol. 54, no. 3, pp. 2606–2615, May 2018.
[37] Y. Peng *et al.*, "PLoRa: A passive long-range data network from ambient LoRa transmissions," in *Proc. Conf. ACM Special Interest Group Data Commun.*, Aug. 2018, pp. 147–160.
[38] H. Nishimoto, Y. Kawahara, and T. Asami, "Prototype implementation of ambient RF energy harvesting wireless sensor networks," in *Proc. IEEE Sensors*, Nov. 2010, pp. 1282–1287.
[39] R. D. Fernandes, N. B. Carvalho, and J. N. Matos, "Design of a battery-free wireless sensor node," in *Proc. IEEE Int. Conf. Comput. Tool (EUROCON)*, Apr. 2011, pp. 1–4.
[40] H. J. Visser and R. J. M. Vullers, "Wireless sensors remotely powered by RF energy," in *Proc. 6th Eur. Conf. Antennas Propag. (EUCAP)*, Mar. 2012, pp. 1–4.
[41] A. N. Parks, A. P. Sample, Y. Zhao, and J. R. Smith, "A wireless sensing platform utilizing ambient RF energy," in *Proc. Power IEEE Top. Conf. Amplif. Wireless Radio Appl. (PAWR)*, Jan. 2013, pp. 160–162.
[42] R. J. Vyas, B. B. Cook, Y. Kawahara, and M. M. Tentzeris, "E-WEHP: A batteryless embedded sensor-platform wirelessly powered from ambient digital-TV signals," *IEEE Trans. Microw. Theory Techn.*, vol. 61, no. 6, pp. 2491–2505, Jun. 2013.
[43] Y. Syed, B. G. Hegde, T. V. Prabhakar, M. Manjunath, and K. J. Vinoy, "RF energy harvesting chip powered sensor node," in *Proc. IEEE Int. Conf. Electron., Circuits Syst. (ICECS)*, Dec. 2016, pp. 748–751.
[44] R. La Rosa, C. Trigona, G. Zoppi, C. A. Di Carlo, L. Di Donato, and G. Sorbello, "RF energy scavenger for battery-free wireless sensor nodes," in *Proc. IEEE Int. Instrum. Meas. Technol. Conf. (I2MTC)*, May 2018, pp. 1–5.
[45] J. Janhunen, K. Mikhaylov, J. Petäjäjärvi, and M. Sonkki, "Wireless energy transfer powered wireless sensor node for green IoT: Design, implementation and evaluation," *Sensors*, vol. 19, no. 1, pp. 90–111, 2019.
[46] S. G. N. Murthy, "Batteryless Wireless RFID based embedded sensors for long term monitoring of reinforced concrete structures," in *Proc. Int. Symp. Non-Destruct. Test. Civil Eng. (NDT-CE)*, Berlin, Germany, Sep. 2015, pp. 15–17.
[47] J. Zhang, G. Tian, A. Marindra, A. Sunny, and A. Zhao, "A review of passive RFID tag antenna-based sensors and systems for structural health monitoring applications," *Sensors*, vol. 17, no. 2, pp. 265–297, 2017.

GAËL LOUBET was born in Toulouse, France, in 1994. He received the Engineering Diploma degree in electronics and automation engineering from the National Institute of Applied Sciences, Toulouse, in 2017, where he is currently pursuing the Ph.D. degree in micro- and nano-systems for communications. He has authored one article in refereed journals. His research interests include communicating materials paradigm, electromagnetic wireless power transfer, wireless communication for the Internet-of-Things applications, and wireless sensor networks for structural health monitoring applications.

ALEXANDRU TAKACS (M'12) was born in Simleu Silvaniei, Romania, in 1975. He received the Engineer Diploma degree in electronic engineering from the Military Technical Academy, Bucharest, Romania, in 1999, and the master's and Ph.D. degrees in microwave and optical communications from the National Polytechnic Institute of Toulouse, Toulouse, France, in 2000 and 2004, respectively. From 2004 to 2007, he was a Lecturer with the Military Technical Academy of Bucharest and an Associate Researcher with the Microtechnology Institute of Bucharest. From 2008 to 2010, he held a Postdoctoral position at the Laboratory for Analysis and Architecture of Systems (LAAS), National Center for Scientific Research (CNRS), Toulouse. In 2011, he was an R&D RF Engineer with Continental Automotive SAS France, where he was in the charge of antenna design and automotive electromagnetic simulation. Since 2012, he has been an Associate Professor with Paul Sabatier University, Toulouse, where he performs research within LAAS-CNRS. He has authored or co-authored one book, one book chapter, 15 papers in refereed journals, and over 70 communications in international symposium proceedings. His research interests include the design of microwave and RF circuits, energy harvesting and wireless power transfer, microelectromechanical systems circuits and systems, small antenna design, electromagnetic simulation techniques, and optimization methods.

DANIELA DRAGOMIRESCU (M'96–SM'15) received the Engineering degree (*magna cum laude*) from the Polytechnic University of Bucharest, Romania, in 1996, the M.Sc. degree in circuits design from Paul Sabatier University, France, in 1997, and the Ph.D. degree (*magna cum laude*) from the University of Toulouse, France, in 2001. She was a French Government Fellow with the Churchill College, University of Cambridge, in 2014. She is currently a Professor with the University of Toulouse, INSA Toulouse, and the LAAS-CNRS Laboratory. He has been the Head of the Microwave and Photonics Systems Department, LAAS-CNRS Laboratory, since 2015. She has been the Dean of the Electrical and Computer Engineering Department, INSA Toulouse, since 2017. She is conducting research in the area of wireless communications with a special focus on wireless sensor networks. She has published more than 80 papers in journals and conferences proceedings and authored seven academic courses. She holds two patents. She was also involved in many national and European research projects in the area of wireless communication. She is the IEEE Solid States Circuits French Chapter Chair. She received the French National Research Agency Grant for Young Investigator in 2005, which supported her in setting up the team in the wireless sensor network area. She was a coordinator of one of the nine French NanoInnov Projects, called Nanocomm on Reconfigurable Wireless Nano-Sensors Networks.